

## Locating a Damage in an Aluminum Plate using Lamb Waves

Faez. A. Masurkar and Nitesh. P. Yelve

<sup>1</sup>*Department of mechanical Engineering, Vishwaniketan Institute of Management Entrepreneurship and Engineering technology, Khalapur, Navi Mumbai-410202, Maharashtra, India.*

*Mob: 08237269549, masurkarf@yahoo.com*

<sup>2</sup>*Department of Mechanical Engineering, Fr. Conceicao Rodrigues Institute of Technology, Vashi, Navi Mumbai- 400 703, Maharashtra, India.*

### **Abstract**

In the present study, Experiments are carried out on an Aluminium (Al) plate with a damage, using Lamb waves and an array of four Piezoelectric Wafer (PW) transducers bonded onto it. The PW transducers are used to actuate and sense Lamb waves. These transducers are small in sizes and cost effective. The data received from the experiments, is further processed using a new algorithm developed by the authors, in order to locate the damage. The damage location is obtained as a small enclosed area formed by the intersection of various curves generated by the algorithm using the data received from the experiments. The damage location is further refined in this enclosed area using the Lagrange optimization method. The results obtained are fairly well. Thus, the present method is capable of locating a damage in plate structures using minimal number of transducers.

**Keywords:** Lamb waves, PW transducers, Locating a damage and optimization.

### **1. Introduction**

Modern structures, particularly those with military applications, are characterized by complexity and greater performance demands, which together with financial and safety limitations make the completion of present designs challenging. Many times, material selection, design, and safety factors must all be combined so as to create a safe, light structure with low initial and maintenance costs. First stages of failure for critical components should be identified as soon as possible, and preferably with low cost, so as to have adequate time for the appropriate repair within an affordable budget to ensure safety and reliability of the system. Furthermore, damage progression monitoring allows estimates of remaining life and helps establish inspection and maintenance intervals.

A variety of defect identification techniques have been developed over the years which include optical, liquid penetrant, magnetic particles, ultrasonic and eddy currents inspection techniques. The majority of these techniques are time-consuming, expensive and require special treatment of the structure, such as disassembly of some parts. Moreover, In general, they are not used to identify damage in real time. The need for real-time, low-cost damage detection, together with the limitations of traditional inspection techniques and the technological improvement in embedded actuators, sensors, reasoning algorithms, and life-prediction methodologies, support the non-destructive evaluation methods under the heading Structural Health Monitoring (SHM). SHM can be described as a continuous, autonomous in-service monitoring of a structure by means of embedded or attached sensors [1].

Among SHM techniques, Lamb waves have been investigated for a number of years because these waves of an elastic type can efficiently travel long distances, and their propagation is affected by cracks and other defects in a structure. Thus, the generation and sensing of these waves in a structure can yield information on the state of

structural damage. This information can then be used to assess system reliability, residual strength, and/or remaining life. Cawley *et al.* [2] realized the attractiveness of using Lamb waves for the inspection of large areas due to their capabilities of propagating long distances.

They discussed that the key for the successful application of the method is the proper excitation of a single mode at a frequency located in a near non-dispersive region. Lowe *et al.* [3] studied issues on Lamb wave sensitivity to defects and optimum selection of modes as related to defect size and the strength of wave reflections. Other studies have focused on sensitivity issues to detect certain forms of damage. Zhu *et al.* [4] documented an experimental study of hidden corrosion detection using ultrasonic guided waves. Chang *et al.* [5] observed that when Lamb waves pass through a region with cracks or material loss, some energy is reflected back due to back scattering and the transmitted waves are modified due to forward scattering. The presence of material loss, cracks or other flaws in the path of the incident Lamb waves can be detected and, in principle, characterized by analyzing the characteristics of the reflected and transmitted waves. Tui *et al.* [6] proposed the elliptical loci method for crack detection with the help of four PW's placed in a square grid configuration. Several loci are constructed based on the time of flights (TOF's) of the wave reflected from the crack. Su *et al.* [7] utilized sets of nonlinear equations established with time lags via the actuator sensor paths and thereafter an optimization method is employed to solve those nonlinear equations. Nevertheless, solving the nonlinear equations is not computationally efficient. Wang *et al.* [8] proposed a method to detect damages in the composite and the concrete materials with the help of TOF's of the wave scattered from the damage. Yuan *et al.* [9] developed a technique to locate damage in an isotropic plate based on the energy propagation of Lamb waves.

The present research focusses on locating a damage in an aluminium plate based on a new algorithm developed by the authors. The information about the arrival time (time from the actuator to the damage and then from damage to the sensor) is obtained by processing the residual signal using Wavelet transform (WT), which is further used with the proposed algorithm to obtain an enclosed area where the probability of damage presence is very high. Further, Optimization is carried out within this area to give a fair accuracy to damage location. The results show that the damage location predicted by the method presented here is very close to the actual location.

## **2. Fundamentals of Lamb waves**

Lamb wave is a type of elastic perturbation propagating in a solid plate with traction free boundaries on their both the surfaces [1-3,11]. This type of wave phenomenon was first described in theory by Horace [11] in 1917. Lamb wave propagates in two modes, symmetric (*S*) and antisymmetric (*A*). The Rayleigh-Lamb wave equation for the symmetric and antisymmetric modes in an isotropic plate is given by [1-3,10,11].

$$\frac{\tan(qh)}{\tan(ph)} = -\frac{4k^2qh}{(k^2-q^2)^2} \text{ and } \frac{\tan(qh)}{\tan(ph)} = -\frac{(k^2-q^2)^2}{4k^2qh}$$

where,  $h$  is the plate thickness,  $k$  is wave number, and

$$p^2 = \frac{\omega^2}{c_L^2} - k^2 \text{ and } q^2 = \frac{\omega^2}{c_T^2} - k^2.$$

$C_L$  is the longitudinal velocity of modes given by  $C_L = (\lambda + 2\mu)/\rho$  and  $C_T$  is the transverse velocity of the modes given by  $C_T = \mu/\rho$ ,  $k = \omega/C_p$ ,  $\lambda = E\nu/((1-2\nu)(1+\nu))$  and  $\mu = E/(2(1+\nu))$  are known as Lamé constants,  $\rho$  is the density,  $E$  is the Young's modulus,  $\nu$  is Poisson's ratio,  $C_p$  is the phase velocity, and  $\omega$  is the wave circular frequency. In the present study, the group velocity is calculated using the relation [12],

$$C_g = C_p \left[ 1 - \frac{f}{c_p} \frac{\partial c_p}{\partial f} \right]^{-1}.$$

The Rayleigh-Lamb equations are solved numerically using bisection algorithm leading to the so-called dispersion characteristics. Figs.1 and 2 show the phase and the group velocity dispersion curves of Lamb waves in an aluminum plate. The dispersion curves for aluminium plate show that at low frequency-thickness product,

only two fundamental modes,  $S_0$  and  $A_0$  can propagate. However, as the frequency-thickness product increases, more number of modes may exist and the interpretation of signals becomes more complicated. Furthermore, because of this dispersive nature of the modes, the shape of a pulse signal containing a band of the frequencies changes with the propagation time and distance, making the measurement of their arrival times difficult. The multiple-mode and dispersive characteristics of Lamb waves complicate signal interpretation for damage identification.

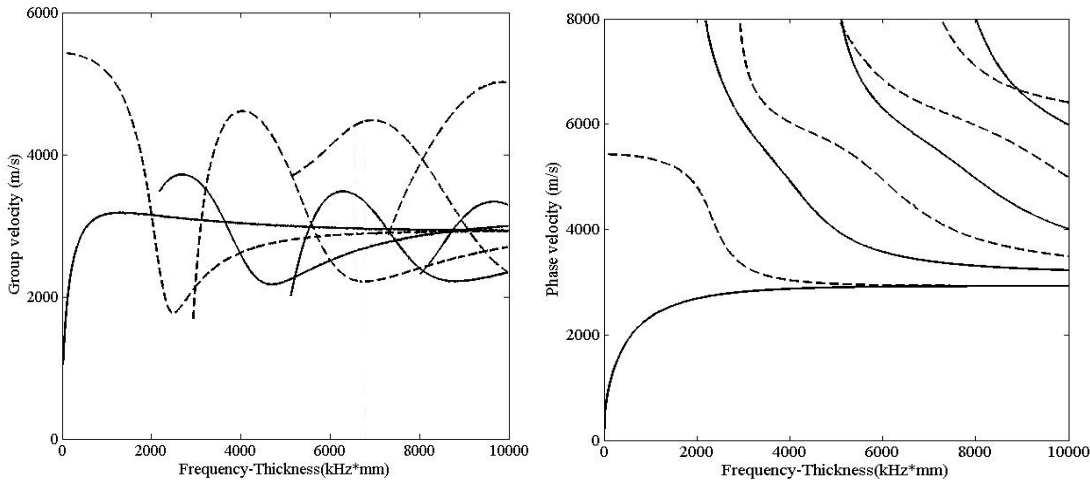


Fig 1. Phase velocity dispersion curve for an aluminium plate Fig 2 Group velocity dispersion curve for an aluminium plate (Continuous lines show A modes and dotted lines show S modes) (Continuous lines show A modes and dotted lines show S modes)

In general, fundamental  $A_0$  and  $S_0$  modes are commonly used for damage detection.  $S_0$  mode is faster and has much lower attenuation than  $A_0$  mode and therefore can propagate longer distance. On the other hand,  $A_0$  mode is more sensitive to small damages because of its shorter wavelength. Therefore, in the present study, interaction of  $A_0$  mode with the damage is studied.

### 3 Experimentation

The current section deals with experimental set up, specimen, comparison of dispersion curves and selection of Excitation frequency.

#### 3.1 Experimental set up

The experimental setup as shown in Fig. 3, consists of Tektronix AFG 3021B single channel arbitrary function generator, Tektronix TDS 1002B two channel digital storage oscilloscope, and a computer having online connection with the oscilloscope. In the experimental work, PW transducers are used to actuate and receive Lamb wave in an aluminium plate.

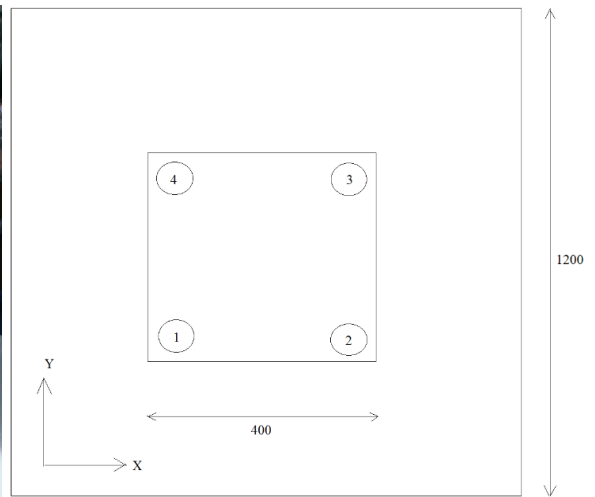
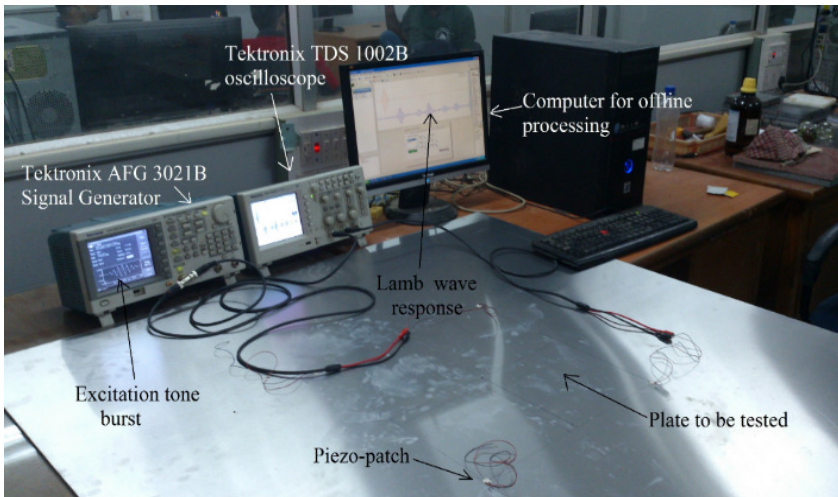


Fig.3 Experimental setup Fig.4 Specimen Geometry

The PW transducers of 10 mm diameter and 0.5 mm thickness are used for actuation and sensing of Lamb wave. These are bonded onto the plates using a commercially available epoxy based adhesive. The PW circular patches named  $S_1$ ,  $S_2$ ,  $S_3$ , and  $S_4$  are bonded at locations (400, 400), (800, 400), (800, 800), (400, 800) respectively onto the plate with the planar form dimensions as 1200 mm  $\times$  1200 mm as shown schematically in Fig. 4.

### **3.2 Specimen :**

The specimen under study is a 1 mm thick sheet of Al-5052 aluminium alloy having modulus of Elasticity of 70.3 GPa, Poisson's ratio of 0.33 and density of 2680 kg/m<sup>3</sup>.

### **3.3 Actuation and sensing :**

Excitation tone burst used is a 8.5 cycle sine wave windowed by Gaussian function as shown in Fig.5. Gaussian windowing function is used here because it produces a tone burst which has narrow frequency bandwidth with less sidebands. The number of cycles considered for the tone burst is 8.5, because for these many cycles, the Lamb wave modes are seen well separated, the frequency bandwidth is less, and the half cycle in the tone burst brings the peak amplitude at the Centre which helps in calculating group velocity. The tone burst with 8.5 cycles and 10 Volt (peak to peak) supplied to PW actuator is found to possess sufficient energy required for exciting the range of frequencies as shown in Fig.6. The received Lamb wave signals at the PW sensor are shown by the oscilloscope and are sent to computer for further offline signal processing [13,14].

### **3.4 Comparison of Dispersion curves :**

Experimentally obtained group velocities are compared with those obtained analytically and are found to be in good agreement as shown in the Figs.6. This shows that there is effective actuation and sensing of Lamb wave in the aluminium plate.

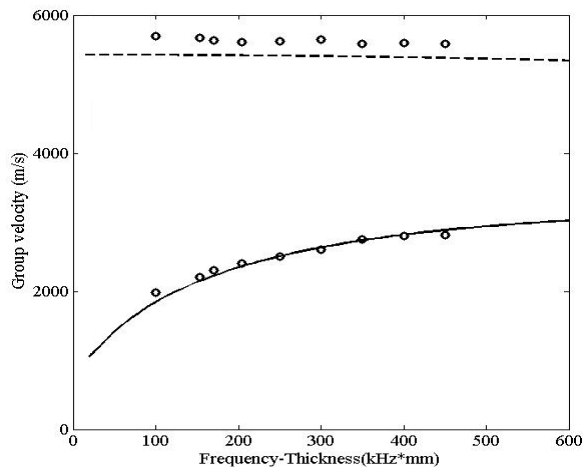
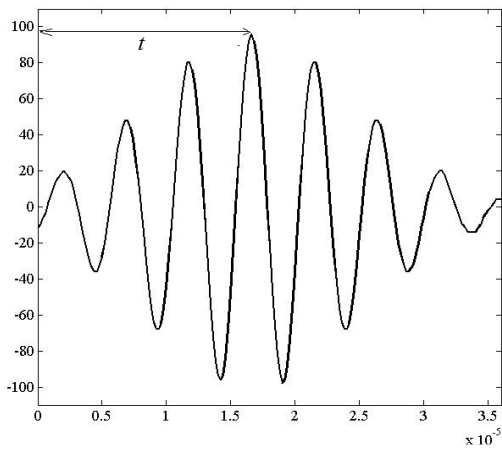


Fig.5. Excitation pulse Fig.6 Comparison of analytical and experimental dispersion curves for a aluminium plate (Continuous line shows  $A_0$  mode and dotted line shows  $S_0$  mode, o shows experimental results)

### 3.5 Selection of Excitation frequency

The computed dispersion curves are used as a guideline to select the excitation frequency. Firstly, the excitation frequency of the tone burst signal should be low enough, where only  $A_0$  and  $S_0$  mode can propagate. As suggested by Giurgiutiu [10] and also reported in [12], damage detection should be carried out at the center frequency where the peak wave amplitude ratio between the  $S_0$  mode and the  $A_0$  mode is maximum. This center frequency is referred to as the ‘sweet spot’.

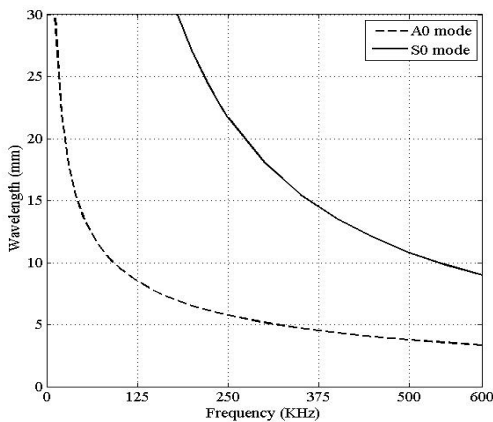


Fig.7 Wavelength dispersion

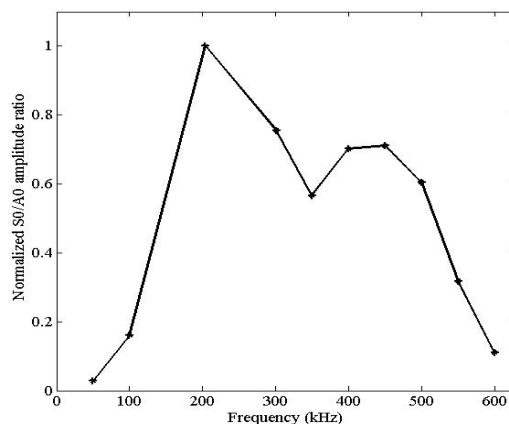


Fig.8 Dispersion of  $S_0/A_0$  ratio

The study done by Giurgiutiu [10] showed that when the diameter of PZT actuator is equal to odd intermultiple of half wavelength of the particular Lamb mode, strong voltage response for the corresponding Lamb mode will be produced, whereas when the diameter of PZT actuator is equal to even integer multiple of half wavelength of Lamb modes, very weak voltage response will be generated. At 204 kHz, the wavelength for  $A_0$  mode is 6.545 mm and for  $S_0$  mode is 27.51 mm as can be seen from the Fig.7, and therefore  $S_0$  mode can be dominantly generated. Hence, at this frequency, maximum amplitude ratio will be obtained. The expected ‘sweet spot’ frequencies is identified to be 204 kHz for the aluminium as shown in the Fig.8.

Further, Experiments are performed on healthy and damaged plates with different pairing configurations of actuators and sensors. Each time one sensor acts as an actuator while the remaining three acts as sensors. Hence, For healthy and damaged state, 12 responses are obtained each. Damage is created in the same healthy plate after obtaining the healthy state responses. Signal processing is carried out for each response using wavelet transform which is discussed in following section 4.

#### 4. Signal Processing :

The present work uses the proposed algorithm for locating the damage in the aluminium plate. The algorithm requires the arrival times as the main input for locating the damage. Signal processing using Continuous wavelet transform (CWT) is used here for getting the arrival times data which is discussed in the following subsection.

##### 4.1 Continuous Wavelet transform (CWT)

According to Daubechies, CWT is defined as [13,14],

$$W(s,p)=\frac{1}{\sqrt{s}} \int_{-\infty}^{\infty} f(t)\varphi * \left(\frac{t-p}{s}\right) dt$$

where,  $f(t)$  is the input signal,  $s$  and  $p$  are real numbers called scale (or dilation) and position, respectively.  $W(s,p)$  are the wavelet coefficients of the function  $f(t)$ , and  $\varphi\left(\frac{t-p}{s}\right)$  is the wavelet function while the symbol  $*$  denotes the complex conjugation. A CWT allows the division of a continuous time function into wavelets and the construction of a time-frequency representation of a given input signal and is used here to get the arrival times. In the present study, the wavelet transform is carried out in a freeware AGU Vallen wavelet software.

Here, more emphasis is given on residual signal (difference between healthy and damage signal) because it contains only the back-scattered reflection coming from the damage and also from multiple scattering between the damage and the boundaries in the structure [5]. Lamb wave is highly sensitive to the presence of any damages and its propagation is affected by the presence of such discontinuities. This irregularities are revealed by peaks as can be seen in Fig.9. The arrival times are obtained pertaining to the peaks and are further used in the algorithm which is discussed in the following subsection.

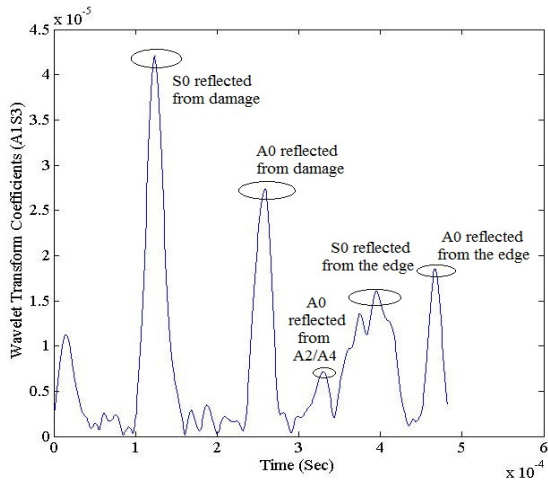


Fig.9 Wavelet transform coefficients

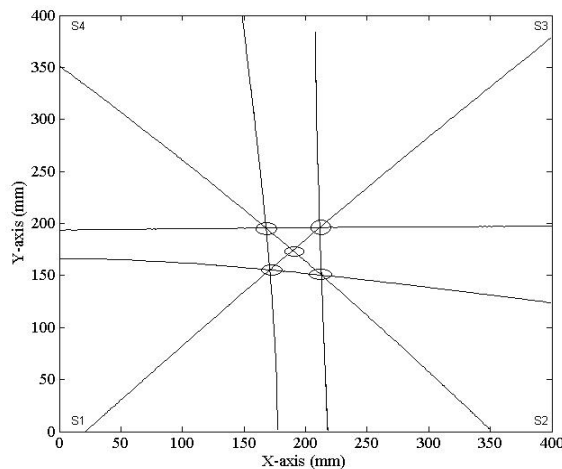


Fig.10 Algorithm output

##### 4.2 The Algorithm :

Consider two sensors  $S_2$  and  $S_3$  located at  $(S_{2x}$  and  $S_{2y})$  and  $(S_{3x}$  and  $S_{3y})$  with 'V' being the velocity of the wave in the plate. Let  $t_2$  and  $t_3$  be the time taken by the wave generated from the actuator  $A_1$  to reach the damage  $d$  and further to the sensors  $S_2$  and  $S_3$  respectively. The time taken by the wave to reach the two sensors from the damage is proportional to the distance difference between the damage and the sensors. Therefore, the governing equation is given by,

$$(D(A_1 \text{ to } d)+D(d \text{ to } S_2))- (D(A_1 \text{ to } d)+D(d \text{ to } S_3))=Vx((t_2-t)-(t_3-t))[A]$$

If a damaged  $d$  is created at a location  $d_x$  and  $d_y$  in a planar surface then the distance between the Actuator  $A_1$  to damage  $d$  is given by,

$$D(A_1 \text{ to } d) = \sqrt{(S_{1x} - d_x)^2 + (S_{1y} - d_y)^2},$$

and the distance from the damage to sensor  $S_2$  is given by,

$$D(d \text{ to } S_2) = \sqrt{(d_x - S_{2x})^2 + (d_y - S_{2y})^2}.$$

where  $t$  is the input/reference time which needs to be subtracted from the arrival time as shown in the Fig.5,  $D$  refers to distances. Hence, The equation Eq. [A] reduces to

$$D(d \text{ to } S_2) - D(d \text{ to } S_3) = Vx(t_2 - t_3)$$

The above equation gives a curve pertaining to the combination of  $A_1S_2$  and  $A_1S_3$ , which means  $S_1$  acting as actuator and  $S_2$  receiving the signal. Similarly, different curves can be obtained for other combinations of actuators and sensors. The generated curves give the damage location as an enclosed area as shown in Fig.10. The location is further refined in this area using the Optimization method discussed in the following subsections.

## **5. Optimization :**

The algorithm generates six curves pertaining to difference in arrival times for  $S_1-S_2$ ,  $S_2-S_3$ ,  $S_3-S_4$ ,  $S_4-S_1$ ,  $S_1-S_3$  and  $S_2-S_4$  which results in an enclosed area as shown in the Fig.10. The probability of damage presence in

this enclosed area is very high. The present work uses Euclidean and Lagrange optimization techniques to refine the damage location within this area and is discussed in the following subsections.

### **5.1. Euclidean Optimization**

In this method, the curves generated by the algorithm are approximated by lines. Let  $P(x_0, y_0)$  be the point from which the shortest distance to the approximated lines of the form  $y = mx + k$  is to be determined. The equation of normal of that line which passes through this point is given by;

$$y = \frac{x_0 - x}{m} + y_0;$$

The point at which these two lines intersect, is the closest point on the original line to the point  $P$ .

Hence;

$$mx + k = \frac{x_0 - x}{m} + y_0;$$

Solving for  $x$ ;

$$x = \frac{x_0 + my_0 - mk}{m^2 + 1};$$

The  $y$  co-ordinate of the point of intersection can be found by substituting this value of  $x$  into the equation of original line.

$$y = m \left( \frac{x_0 + my_0 - mk}{m^2 + 1} \right) + k;$$

Using the equation for finding distance between two points;

$$d = \sqrt{(x_2 - x_1)^2 + (y_2 - y_1)^2}$$

We can deduce that the equation for the shortest distance between a line and a point is the following;

$$d = \sqrt{\left( \frac{x_0 + my_0 - mk}{m^2 + 1} - x_0 \right)^2 + \left( m \frac{x_0 + my_0 - mk}{m^2 + 1} + k - y_0 \right)^2}$$

The following method can be useful wherein we have n lines, which are non-intersecting at a single point and we need to find the optimum solution. In the present work, we have formulated an objective function in such a way that the sum of the minimum distance from this point to all the lines is minimum.

Mathematically,

$$F = \min\{\sum_{i=1}^n d_i | (x^*, y^*)\};$$

Where,  $d_i$  is the minimum distance from the point to the line, n is the number of lines and  $x^*, y^*$  is the optimum solution reached.

## **5.2. Lagrange Optimization**

In mathematical optimization, the method Lagrange multipliers is a strategy for finding local maxima and minima of a function subject to equality constraints. Let us consider the following optimization problem,

$$\text{Minimize } f(x, y)$$

$$\text{s.t. } g(x, y) = 0$$

We need here both  $f$  and  $g$  to have continuous first partial derivatives. Let us introduce a new variable  $\lambda$  called the Lagrange multiplier. The Lagrange function will be formulated as;

$$L(x, y, \lambda) = f(x, y) + \lambda g(x, y)$$

where;  $f(x, y) = \sqrt{(x - x_0)^2 + (y - y_0)^2}$  and

$g(x, y) = ax^3 + bx^2 + cx + d$  is a cubic curve which will almost imitate the curve generated by the algorithm unlikely in the case of Euclidean optimization wherein the curves are approximated as straight lines. If  $f(x^*, y^*)$  is the optimum of  $f(x, y)$ , then there exists a  $\lambda^*$  such that  $x^*, y^*$  and  $\lambda^*$  is a stationary point for the Lagrange function.

The stationary points are those where the partial derivatives of Lagrange function are zero.

$$\frac{dL}{dx} = 0, \frac{dL}{dy} = 0, \frac{dL}{d\lambda} = 0$$

The above conditions will give three equations which needs to be solved simultaneously to get optimum  $x^*, y^*$  and  $\lambda^*$ . The distance between the optimum point and the concerned point can be found using;

$$d = \sqrt{(x_0 - x^*)^2 + (y_0 - y^*)^2}$$

In the present work, we minimize the sum of the distances from each point to all the curves similar to Euclidean optimization.

## **6. Results**

The location of damage obtained through the Euclidean optimization is found to be (183.3, 169.2) mm having an error of 2.53 % with the actual location (182, 180) mm as shown in the Fig.11. In case of Lagrange Optimization method, the located predicted is found to be (182.1, 177.4) mm with an error of 0.4 %. It is seen that the accuracy is improved in the latter, as the regression is cubic in the latter and linear in the former. The colorbar shows the functional values in mm.



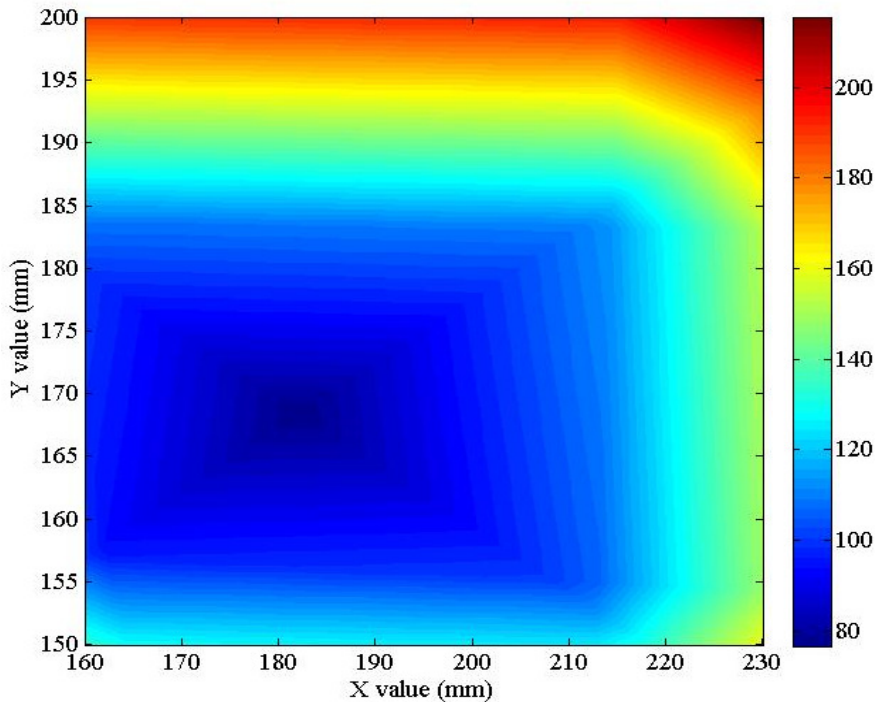


Fig.11 Damage location predicted by the Euclidean Optimization

## 7. Conclusions

In this work, the interaction of  $A_0$ Lamb wave mode with the damage in an aluminium plate is studied. Lamb wave responses are obtained experimentally for a healthy plate at different frequencies and group velocities are calculated. These group velocities are compared with those obtained analytically and found to be in close agreement. This confirms effective actuation and sensing of Lamb wave in the plate.

Experiments are carried out on the healthy and the damaged state of aluminium plate, and the Lamb wave responses are recorded. Arrival times of the waves are extracted for this Lamb wave data using wavelet transform. Further, the proposed algorithm is used to locate the damage in the plate as an enclosed area. The location is further refined within this area using the Euclidean and Lagrange optimization schemes. The optimized damage location reduces the error between the actual and predicted location using algorithm. It can be finally concluded that, as the degree of fit for the curves increases, Error percentage in damage location reduces.

## 8. References

- [1] H. Speckmann, H. Roesner, "Structural Health Monitoring: A Contribution to the Intelligent Aircraft Structure," *Proceeding of ECNDT 2006*, 9th European Conference on NDT, Berlin, Germany, September 2006.
- [2] P. Cawley, D. Alleyne, "The use of Lamb waves for the long range inspection of large structures," *Ultrasonics* 34, 1996, 287-290.
- [3] M.J.S Lowe, D.N. Alleyne, and P. Cawley, "Defect detection in pipes using guided waves," *Ultrasonics* 36, 1998, 147-154.
- [4] W. Zhu, J.L. Rose, J.N. Barshinger, V.S. Agrawala, "Ultrasonic guided wave NDT for hidden corrosion detection," *Res. Nondestr. Eval.* (1998), 10, 205-225.

**NDE 2015, Hyderabad**  
**November 26-28, 2015**

- [5] Z. Chang and A. Mal, "Scattering of Lamb waves from a rivet hole with edge cracks," *Mechanics of Materials*, 31, 1999, 197-204.
- [6] Tua, P.S., Quek, S.T. and Wang, Q. (2004), "Detection of cracks in plates using piezo-actuated Lamb waves", *Smart Mater. Struct.*, 13(4), 643-660.
- [7] Su, Z.Q., Ye, L. and Bu, X.Z. (2002), "A damage identification technique for CF/EP composite laminates using distributed piezoelectric transducers", *Compos. Struct.*, 57(1-4), 465-471.
- [8] Wang, C.S.F. and Chang, F.K. (2001), "Structural health monitoring from fiber-reinforced composites to Steel reinforced concrete", *Smart Mater. Struct.*, 10(3), 548-552.
- [9] Wang, L. and Yuan, F.G. (2007), "Active damage localization technique based on energy propagation of Lamb waves", *Smart Struct. Syst.*, 3(2), 201-207.
- [10] Giurgiutiu, V., Zagari, A. and Bao, J.J. (2002), "Piezoelectric wafer embedded active sensors for aging aircraft structural health monitoring", *Structural Health Monitoring*, 1(1), 41-61.
- [11] Zhongqing, S., Lin, Y. and Ye, L., "Guided Lamb waves for identification of damage in composite structures: A review," *Journal of sound and vibration*, DOI:10.1016/j.jsv.2006.01.020, (2006).
- [12] Y Lu, X Wang, J Tang and Y Ding, "Damage detection using piezoelectric transducers and the Lamb wave approach: II Robust and Quantitative decision making, *Smart Material Structures*, 17(2008), doi:10.1088/0964-1726/17/2/025034
- [13] Yelve, N. P., Mitra, M. and Mujumdar, P. M., "Spectral damage index for estimation of breathing crack depth in an aluminum plate using nonlinear Lamb wave," *Structural Control and Health Monitoring*, DOI: 10.1002/stc.1604, (2013).
- [14] Yelve, N. P., Mitra, M. and Mujumdar, P. M., "Higher harmonics induced in Lamb wave due to partial debonding of piezoelectric wafer transducers," *NDT & E International*, 63, 21-27 (2014).